

# High-performance differential surface plasmon resonance sensor using quadrant cell photodetector

H. Q. Zhang, S. Boussaad, and N. J. Tao<sup>a)</sup>

*Department of Electrical Engineering and Center for Solid State Electronics Research, Arizona State University, Tempe, Arizona 85287*

(Received 2 July 2002; accepted 24 September 2002)

We describe a simple, stable, and high-resolution surface plasmon resonance (SPR) sensor using a quadrant cell photodetector. The sensor focuses a diode laser through a prism onto a gold film that is divided into two areas, one for reference and the other for sensing analyte. The angular shifts of the SPR generated in the two areas are detected with a quadrant cell photodetector. Because signals from the two areas are produced and detected with the same laser, optics, and photodetector, the difference in the SPR angular shifts eliminates errors due to thermal drift, mechanical noise, and laser fluctuations. It also removes the SPR angular shift due to the change in the refractive index of the bulk solution as an analyte solution is introduced into the sample cell each time, and thus gives an accurate detection of the specific adsorption of analyte. © 2003 American Institute of Physics. [DOI: 10.1063/1.1523649]

## I. INTRODUCTION

Surface plasmon resonance (SPR) has become a powerful analytical tool for various applications.<sup>1-3</sup> It is based on detecting the resonance of surface plasmons, or collective oscillations of electrons, in a metallic film with light.<sup>4,5</sup> Because the resonance condition is extremely sensitive to the refractive index of the medium adjacent to the metallic film, presence of analyte molecules on the surface of the metallic film can be accurately detected. High specificity of SPR sensors is usually achieved by modifying the metal surface with a layer of appropriate ligand molecules to allow specific binding between the analyte and the ligand.<sup>6-8</sup> When operated in the multiwavelength mode,<sup>9-11</sup> the wavelength dependent SPR shift is related to the absorption band of the analyte molecules, thus providing additional information on the identity of the analyte.<sup>12,13</sup> Once molecules bind to the surface, SPR sensors can also be used to study conformational changes of surface bound molecules.<sup>14-18</sup> The current commercially available SPR sensors have good sensitivities but, for many applications, it is desired to have a higher sensitivity SPR sensor. Examples include analyzing extremely dilute sample solutions, detecting trace amount of low molecular weight analyte and studying subtle conformational changes in proteins.

We have recently reported on a simple SPR sensor that achieves high resolution by using a bicell photodetector.<sup>15</sup> The setup allowed us to achieve an angular resolution of  $10^{-5}$  degrees. Because of the extremely high resolution, small mechanical vibration and thermal drifts over a long time become practically the limiting factors that prevented us from studying slow processes. Furthermore, the method cannot discriminate between a specific binding event of an analyte onto the metal surface and a change of the refractive index in the bulk solution. This article describes a highly

sensitive differential SPR sensor with a quadrant photodetector. The sensor remedies most of the problems just mentioned without compromising either resolution or simplicity.

## II. PRINCIPLE

Our setup is based on the widely used Kretschmann configuration, in which a *p*-polarized laser beam is focused through a prism onto the metal film placed on the prism. Because the incident beam is focused, it spans over a range of incident angles depending on the focus distance and beam width. At the so-called resonance angle, the incident light is absorbed by the surface plasmon and the reflection drops to a minimum, which results in a dark thin line known as the SPR dip. The dip shift measures the change of the resonance angle, which provides a sensitive detection of an analyte on the metal film. So an accurate, rapid, and reliable determination of the SPR dip shift is of the primary importance in the construction of an SPR sensor. A charge coupled device (CCD) and linear diode array (LDA) are often used to record the dip profile from which the dip position is determined by numerical fitting.<sup>19-24</sup>

We have recently replaced the CCD or LDA detectors with a much simpler and more compact bicell photodetector. The reflected light falling onto the two cells of the photodetector is first balanced such that the SPR dip is roughly located near the center of the photodetector. A small shift in the dip position causes an imbalance between the two cells of the bicell photodetector which is detected as a change of intensity, given by  $(A - B)/(A + B)$ , where *A* and *B* are the signals of the two cells. Because the two cells are nearly identical, all common noises, such as laser intensity fluctuations, detected by both cells are subtracted out, thus providing a simple and accurate ( $10^{-5}$  degrees) method to measure the SPR angular shift.

At high resolution, thermal drift due to temperature gradient or mechanical drift due to stress created during optical

<sup>a)</sup>Electronic mail: nongjian.tao@asu.edu

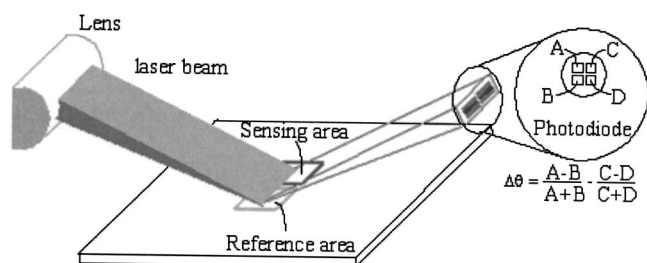


FIG. 1. Schematic representation of the differential SPR setup. A diode laser is focused with a cylindrical lens through a prism onto the gold film supported on the prism (not shown for clarity). The gold film is divided into a sensing area and a reference area. The reflected beams from the two areas have dark lines (SPR dips) when the incident angle is appropriately adjusted. A quadrant cell photodetector simultaneously measures the SPR dips from the reference and sample areas, and the difference signal,  $(A-B)/(A+B) - (C-D)/(C+D)$ , provides an accurate measurement of the specific adsorption of an analyte onto the sample area.

alignment becomes non-negligible. In addition to the noise problem, the change of the solution refractive index due to the introduction of an analyte into the cell can cause a dip shift that overwhelms the shift due to the specific binding of the analyte. This is a longstanding problem in SPR sensors, but it becomes more serious in high-resolution SPR sensors. By dividing the metal film into two separate areas, a non-reactive area as reference and a reactive area for sample analysis,<sup>25-27</sup> both the noise problem and the change of the bulk refractive index are greatly reduced by measuring the difference between the sample and reference signals. This is achieved by focusing the laser beam with a lens on both the sample and reference areas. The resulting SPR dips of sample and reference areas are detected with a quadrant photodetector. In comparison with the previous reference-compensated setups, the sample and reference signals in the present design are originated from the same light source focused with the same optics and detected with nearly identical photocells integrated on the photodetector, which provides effective reduction in thermal drift, mechanical noises, and bulk refractive index effect.

### III. EXPERIMENT

#### A. Instrumentation

Figure 1 schematically shows the SPR setup. A BK7 cylindrical lens (Melles Griot) was used as a prism on which a BK7 glass slide coated with gold film was placed with a refractive index matching fluid. The gold electrode is divided into an active sample area and a reference area. A Teflon cell was mounted on the gold film to hold the sample solution. The laser beam ( $\lambda = 635$  nm, Hitachi) is collimated and then focused with a cylindrical lens into a line equally distributed on both sample and reference areas. Light reflected from the sample and reference areas of the gold film is detected with a quadrant cell photodetector (Advance Photonix). The photocurrents from the four cells (A, B, C, and D) were converted to voltages with a homemade electronic circuit. The circuit calculated the differential  $(A-B)$  and  $(C-D)$  and the sum  $(A+B)$  and  $(C+D)$  signals, which are recorded with a four channel 150 MHz digital oscilloscopes (Yokogawa, DL708). Prior to each measurement, the prism was rotated to bring

the SPR dip at the center of the reflected beam spot, and the quadrant photodetector is adjusted to balance A and B for the sample signal and C and D for the reference signal. The SPR shift due to the specific binding of analyte is obtained by computing the following expression:  $(A-B)/(A+B) - (C-D)/(C+D)$ .

#### B. Fabrication of reference and sample areas on gold film

The gold film ( $\sim 50$  nm thick) is evaporated on a BK7 glass substrate by an ion beam coater (Model 681, Gatan Inc.). Since we chose heavy metal ion detection to demonstrate the SPR sensor, we coated the reference area with a monolayer of 1-dodecanethiol (Aldrich) and the sample area with a monolayer of 3-mercaptopropionic acid using a polydimethylsiloxane (PDMS) stamp. The positively charged metal ions should not bind to the  $-\text{CH}_3$  group but bind to the  $-\text{COO}^-$  group via electrostatic interactions. The reference and sample areas are separated with a gap of  $100 \mu\text{m}$ .

### IV. RESULTS AND DISCUSSION

#### A. Calibration of the quadrant photocell detector

Effective removal of thermal drift, mechanical noise, and bulk refractive index change requires identical four photocells in the quadrant photodetector. Variations between the photocells in the commercial photodetectors are specified to be less than 1%. Additional variations may originate from the amplification circuit that computes quantities,  $(A-B)$ ,  $(A+B)$ ,  $(C-D)$ , and  $(C+D)$ . It is essential to determine the actual difference in the sensitivities of  $(A-B)/(A+B)$  and  $(C-D)/(C+D)$  due to manufacturing errors and signal amplifications. We have calibrated  $(A-B)/(A+B)$  and  $(C-D)/(C+D)$  by introducing into the sample cell various mixtures of water and ethanol. The angular shift due to the consequent change of index of refraction is measured simultaneously by  $(A-B)/(A+B)$  and  $(C-D)/(C+D)$ . We found a linear relationship between  $(A-B)/(A+B)$  and  $(C-D)/(C+D)$ , as shown in Fig. 2. The slope is  $\sim 1.004$ , meaning that the difference between  $(A-B)/(A+B)$  and  $(C-D)/(C+D)$  is as small as 0.04%. Thus, we expect a two orders of magnitude reduction of thermal drift, mechanical noise, and change of the bulk refractive index.

#### B. Thermal drift and mechanical noise

Immediately after mounting the sample cell, mechanical stress, and equilibration of temperature gradient cause a drift in the SPR signal that can last from minutes to hours. This drift is a serious problem for high-resolution ( $< 10^{-3}$  degrees) SPR. We have used a compact design with minimized number of movable components and low thermal expansion material (Invar) in our previous bicell SPR sensor, but still drift is a limiting factor that hampers the application of high-resolution SPR to monitor slow binding processes. In the present sensor, mechanical noise and thermal drift are eliminated with the reference signal. The effectiveness of this differential method is demonstrated in Fig. 3. The drifts recorded in both the sample and reference signals are roughly

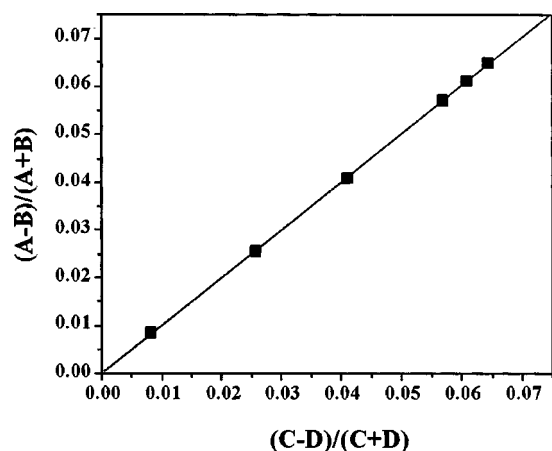


FIG. 2. The response of the sample SPR signal is plotted vs that of the reference signal upon introduction of various concentrations of ethanol in water. Since the sample and reference areas are the same, any difference in their SPR signals would reflect different optics, amplification gain, or gold film thickness. The data show a linear relationship between the sample and reference signals with a slope of 1.004, indicating nearly identical SPR responses of the sample and reference signals.

linear with a small bending near the middle of the plot. By fitting the data with a linear expression, the amount of drift determined from the slope is about  $6 \times 10^{-4}$  degrees/min. After subtracting the drift of the sample signal  $(A-B)/(A+B)$  to that of the reference signal  $(C-D)/(C+D)$ , the linear drift is dramatically reduced to  $3 \times 10^{-7}$  degrees/min. The subtraction of the bending part is less desirable, which is probably due to relative change in the reference and sample areas.

### C. Change of the refractive index of the bulk solution

In order to demonstrate the ability of the differential SPR sensor to eliminate the change of the refractive index of the bulk solution, we have measured the SPR shift by injecting various amounts of  $\text{Pb}(\text{NO}_3)_2$  into the sample cell. Both the sample and reference areas of the gold film were coated with  $\text{CH}_3$ -terminated thiol molecules so that no specific adsorption of  $\text{Pb}^{+2}$  or  $\text{NO}_3^-$  onto the metal surface is expected. The

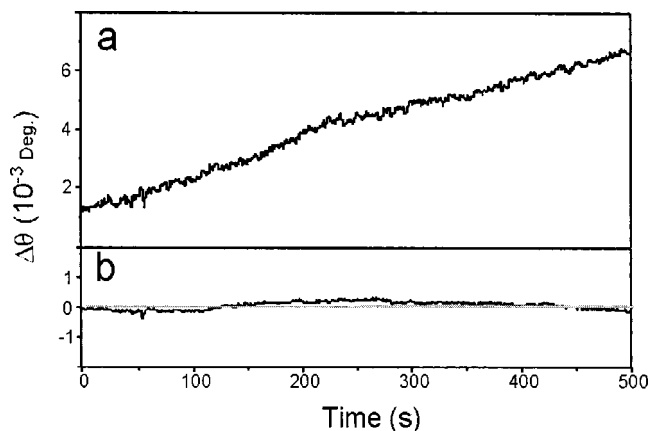


FIG. 3. (a) SPR shift vs time in water recorded immediately after mounting the optics and sample cell. It shows a large drift due to thermal/mechanical drift. (b) After subtracting out the reference signal, the large drift is essentially removed.

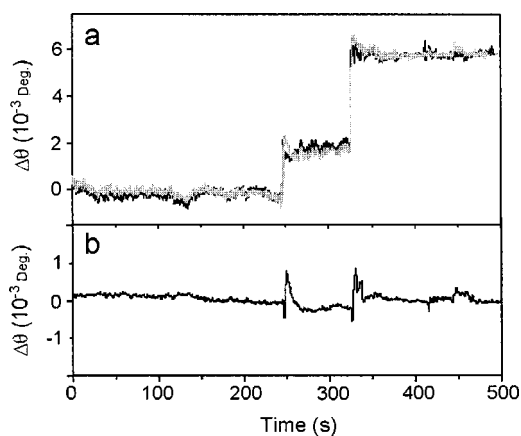


FIG. 4. Effective removal of bulk refractive index influence can be achieved from the differential signal (green line):  $(A-B)/(A+B) - (C-D)/(C+D)$ . Prior to the experiment, the sample cell was filled with  $100 \mu\text{l}$  and then injected with the solution of  $\text{Pb}(\text{NO}_3)_2$ . The final concentrations of  $\text{Pb}(\text{NO}_3)_2$  are indicated as the arrows. The black line is the sample signal,  $(A-B)/(A+B)$  and the gray line is the reference signal,  $(C-D)/(C+D)$ .

introduction of  $\text{Pb}(\text{NO}_3)_2$  into the sample cell causes a step-wise increase in both  $(A-B)/(A+B)$  and  $(C-D)/(C+D)$  signals, due to the change of the refractive index of the bulk solution (Fig. 4). After subtracting the reference signal, no net change in the SPR shift is observed. However, we noticed sharp changes in the SPR shift that coincide with the moments where the solution is introduced into the sample cell. These sharp changes correspond to the inhomogeneous mixing of the added  $\text{Pb}(\text{NO}_3)_2$  with the rest of the solution, which disappear after a uniformed mixing is reached.

### D. Random noises

The present SPR sensor can greatly reduce random noises that cannot be eliminated with the bicell photodetector. Sources of such noises include mechanical vibrations and spatial intensity fluctuations of the laser diode. Figure 5(a) shows the random noise as function of time before subtract-

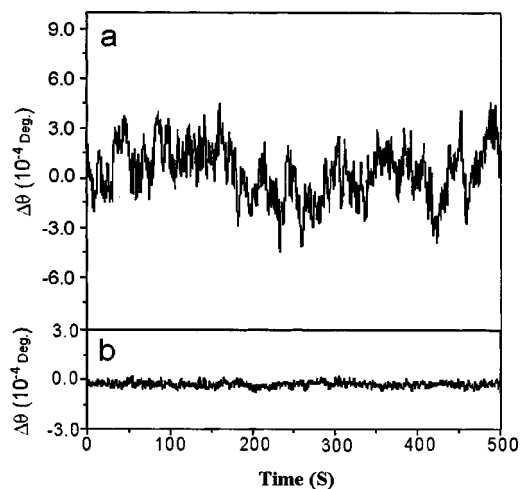


FIG. 5. (a) SPR vs time in water. Systematic thermal and mechanical drift in this measurement is small and the error is dominated by random fluctuations in the signal that might be due to mechanical vibrations. (b) After subtracting the fluctuations with the reference signal, the rms noise level is reduced by one order of magnitude.

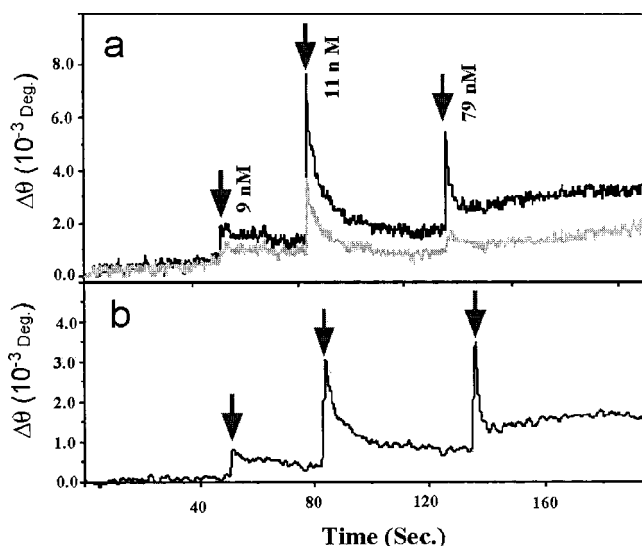


FIG. 6. Detection of specific adsorption of  $Pb^{2+}$  ions. (a) The sample and reference SPR signals upon introduction of various amounts of  $Pb(NO_3)_2$  into the solution cell. The sample signal is the SPR angular shift from the sample region coated with a monolayer of  $COO^-$ -terminated thiol that is ready to bind with  $Pb^{2+}$  ions. The signal also contains the change in the refractive index of the bulk solution. The reference signal is from the area coated with inert  $CH_3$ -terminated thiol layer, which reflects the change in the refractive index only. (b) After subtracting out the reference signal from the sample signal, the specific adsorption of  $Pb^{2+}$  ions is obtained.

ing the reference signal. Thermal drift and mechanical noise are quite small ( $<2 \times 10^{-7}$  degrees/min). The root-mean square (rms) of the random noise is about  $1.5 \times 10^{-4}$  degrees, which is most likely due to mechanical vibrations since the laser intensity fluctuations and electronic noises are much smaller. After subtracting the reference signal, the noise level is reduced to  $\sim 1.5 \times 10^{-5}$  degrees, one order of magnitude better.

### E. Detection of trace amounts of lead ions

SPR has been combined with cyclic voltammograms to detect heavy metals ions.<sup>28,29</sup> Simultaneous sensing of 500 nM lead and copper ion have been demonstrated.<sup>29</sup> We have applied the differential SPR sensor to the detection of heavy metal ions. For this experiment, the reference and sample areas are coated with self-assembled monolayers of 1-dodecanethiol and 3-mercaptopropionic acid, respectively. Metal ions do not bind to  $CH_3$ -terminated 1-dodecanethiol molecules but they are expected to bind to the negatively charged carboxylic groups of the 3-mercaptopropionic acid. The reference area is coated first with 1-dodecanethiol using a PDMS stamp, and then the gold film is placed in the sample cell filled with water. Upon introduction of a drop of 3-mercaptopropionic acid solution (2 mM) into the sample cell, self-assembly of these molecules onto the bare gold surface of the sample area causes a large SPR shift. As expected, the reference signal changed little over the same period of time.

After a stable monolayer of 3-mercaptopropionic acid is formed, we repeatedly flushed the sample cell with water and then introduced various amount of the  $Pb^{2+}$  ions into the

solution. The consequent SPR shifts of the sample and reference areas are shown in Fig. 6. The reference signal reflects changes of the refractive index of the bulk solution, while the sample signal contains both changes of the refractive index of the bulk and binding of  $Pb^{2+}$  ions to  $COO^-$  terminal groups. By subtracting the change of the refractive index of the bulk, the SPR shift due to the binding of heavy metal ions was extracted and plotted in Fig. 6(b). The data shows that 9 nM of  $Pb^{2+}$  ions can result in a  $7 \times 10^{-4}$  degree SPR shift. Because the rms noise achieved with the differential sensor is  $\sim 1.5 \times 10^{-5}$  degrees, the lower detection limit of the sensor is estimated to  $\sim 0.2$  nM or 0.04 ppb of  $Pb^{2+}$  ions assuming a linear relationship between the concentration of ions and the SPR shift at low concentrations.

### ACKNOWLEDGMENTS

Financial support is acknowledged through grants from the EPA (Grant No. R829623) and the NSF (Grant No. CHE-9818073).

- <sup>1</sup>B. Liedberg, C. Nylander, and I. Lundstrom, *Sens. Actuators* **4**, 299 (1983).
- <sup>2</sup>R. J. Fisher and M. Fivash, *Current Biotechnology* **45**, 65 (1994).
- <sup>3</sup>K. Moffat and G. Wagner, *Curr. Opin. Struct. Biol.* **5**, 637 (1995).
- <sup>4</sup>A. Otto, *Z. Phys.* **216**, 398 (1968).
- <sup>5</sup>E. Kretschmann, *Z. Phys.* **241**, 313 (1971).
- <sup>6</sup>I. Lundstrom, *Biosens. Bioelectron.* **9**, 725 (1994).
- <sup>7</sup>J. Homola, S. S. Yee, and G. Gauglitz, *Sens. Actuators B* **54**, 3 (1999).
- <sup>8</sup>M. L. Shank-Retzlaff and S. G. Sligar, *Anal. Chem.* **72**, 4212 (2000).
- <sup>9</sup>I. Pockrand *et al.*, *J. Chem. Phys.* **69**, 4001 (1978).
- <sup>10</sup>K. A. Peterlinz and R. Georgiadis, *Opt. Commun.* **130**, 260 (1996).
- <sup>11</sup>K. A. Peterlinz and R. M. Georgiadis, *J. Am. Chem. Soc.* **119**, 3401 (1997).
- <sup>12</sup>S. Boussaad, J. Pean, and N. J. Tao, *Anal. Chem.* **72**, 222 (2000).
- <sup>13</sup>S. Wang *et al.*, *Anal. Chem.* **72**, 4003 (2000).
- <sup>14</sup>Z. Salamon *et al.*, *Biochemistry* **33**, 13706 (1994).
- <sup>15</sup>N. J. Tao *et al.*, *Rev. Sci. Instrum.* **70**, 4656 (1999).
- <sup>16</sup>T. Ozawa, K. Sasaki, and Y. Umezawa, *Biochim. Biophys. Acta-Protein Struct. Mol. Enzymology* **1434**, 211 (1999).
- <sup>17</sup>H. Sota, Y. Hasegawa, and M. Iwakura, *Anal. Chem.* **70**, 2019 (1998).
- <sup>18</sup>S. Chah *et al.*, *Langmuir* **18**, 314 (2002).
- <sup>19</sup>E. Kretschmann, *Opt. Commun.* **26**, 1 (1978).
- <sup>20</sup>K. Masubara, S. Kawataa, and S. Minami, *Appl. Opt.* **27**, 1160 (1988).
- <sup>21</sup>W. Hickel and W. Knoll, *Thin Solid Films* **199**, 367 (1991).
- <sup>22</sup>K. S. Johnston *et al.*, *Sens. Actuators B* **54**, 80 (1999).
- <sup>23</sup>T. M. Chinowsky, L. S. Jung, and S. S. Yee, *Sens. Actuators B* **54**, 89 (1999).
- <sup>24</sup>K. Johansen *et al.*, *Meas. Sci. Technol.* **11**, 1630 (2000).
- <sup>25</sup>R. P. H. Kooyman *et al.*, *Anal. Chem.* **63**, 83 (1991).
- <sup>26</sup>M. J. O'Brien II *et al.*, *Biosens. Bioelectron.* **14**, 145 (1999).
- <sup>27</sup>G. G. Nenninger *et al.*, *Sens. Actuators B* **51**, 38 (1998).
- <sup>28</sup>C. C. Jung *et al.*, *Sens. Actuators B* **32**, 143 (1996).
- <sup>29</sup>T. M. Chinowsky, S. B. Saban, and S. S. Yee, *Sens. Actuators B* **35**, 37 (1996).